# EXTENSION OF LOW-THRUST PROPULSION TO THE AUTONOMOUS COPLANAR CIRCULAR RESTRICTED FOUR BODY PROBLEM WITH APPLICATION TO FUTURE TROJAN ASTEROID MISSIONS

**Marta Ceccaroni**
Advanced Concepts Space Laboratory, Glasgow, UK
marta.ceccaroni@strath.ac.uk

James Biggs
Advanced Concepts Space Laboratory, Glasgow, UK
james.biggs@strath.ac.uk

An Autonomous Coplanar Circular Restricted Four Body Problem (CRFBP) is considered, where the massless body is a low-thrust spacecraft. "Natural" and "artificial" (i.e. created with the use of continuous low-thrust propulsion) equilibrium solutions are identified, that have the potential to be exploited in future science missions. Results show that, with zero thrust, there are unstable equilibrium points close to the third primary. However, artificial equilibrium points, displaced from the natural ones, can be generated with the use of constant low-thrust. Furthermore, these points are proved to be stable in certain regions about the third primary mass. This is particularly advantageous since it means that it would be possible to continuously maintain a spacecraft about these strategic observation points, close to the smaller primary, without the need for state feedback control.
The Sun-Jupiter-Trojan Asteroid-Spacecraft system is considered, as a particular case of the Autonomous Coplanar CRFBP. Curves of artificial equilibrium points are then identified. Furthermore, the stability analysis of these points reveals the region where they are stable. In this region four bounded orbits close to the Asteroid are proved to exist, that can be reached and maintained with a constant low-thrust lower than $10\mu N$.

**Key words:** Four Body Problems · Low-thrust Propulsion · $L_4$ · Trojan Asteroid

## I. INTRODUCTION

The use of continuous low-thrust propulsion in four body systems could enable a range of potential applications for several fields such as space physics, human exploration, planetary science, asteroid observation and many more.

The present studies on the dynamics of four body problem fall into two general categories:

- where the CRFBP is analyzed as a perturbed Three Body Problem (Hill's approximation). In this case the fourth body is set to be at a large distance from the other assumed three bodies such that it can be considered a perturbation.
  Two examples of this case can be found in Scheeres [1], and the bicircular model considered by Cronin et al.[2], where both models are used to approximate the dynamics of the Sun-Earth-Moon-Spacecraft system;

- where two or three of the primary masses are set to be equal and the planets are in a particular configuration such as the Symmetric, Collinear CRFBP (see [3] or [4]). Generally speaking these systems are motivated by mathematical interest rather than a particular application.

On the other hand, the use of continuous low-thrust propulsion, has so far been confined to two and three-body systems. Space mission design for low thrust spacecraft has been extensively investigated from the late 1990's. So far the two major types of low-thrust propulsion, which have been studied in this context, are solar sails and solar electric propulsion (SEP), the latter considered in this paper.
Research on this topic are, at present, mainly focussed on finding artificial equilibria as in [5], [6] or [7], on generating periodic halo orbits (see, for example, [8], [9] or [10]), or on the systematic cataloguing of non-Keplerian orbits as in [11].

In this paper the interaction between these two relatively new topics is considered and explored both for mathematical interest as well as to identify possible applications for mission design.
To this end an Autonomous Coplanar CRFBP is analy-

zed, with the objective of identifying completely new orbits for future mission applications.
A low-thrust spacecraft is assumed, on the basis of the technical capability of the QinetiQ thrusters [12], which can generate a thrust of approximately $250mN$. Moreover we assume a capability of $300mN$ maximum thrust to account for feasible future advances in low-thrust propulsion systems.

Results show that, with zero thrust, there are unstable equilibrium points close to the third primary. However, artificial equilibrium points, displaced from the natural ones, can be generated with the use of constant low-thrust. Furthermore, these points are proved to be stable in certain regions about the smaller primary. This is particularly advantageous since it means that it would be possible to maintain a spacecraft around strategic observation points about the third primary continuously without the need for state feedback control.

Finally, the particular case of the Sun-Jupiter-Asteroid-Spacecraft Autonomous Coplanar CRFBP is analyzed. In this case the third primary mass is taken to be small to reflect estimates of asteroid masses predicted to be trapped at the triangular Lagrangian points of the Sun-Jupiter-Spacecraft system. Curves of artificial equilibrium points are then identified. The stability analysis of these points reveal the region where they are stable.

This investigation could potentially be useful for designing missions to the Jupiter Trojans. This set of asteroids, captured around the $L_4$ and $L_5$ points of the Sun-Jupiter-Spacecraft system, has been recognized as present target for space science missions; furthermore, understanding them may lead to clues to the origin and dynamical evolution of Jupiter itself [13]. Currently, the Trojan Asteroids are completely unexplored and largely unknown and any visit by a spacecraft will revolutionize our current understanding of these bodies [14]. Moreover, this paper highlights the possibility to maintain strategic observation points close to a Jovian Trojan with reduced requirements on fuel and without the need for a state feedback control.

## II. THE AUTONOMOUS COPLANAR CRFBP

The Autonomous Coplanar Circular Restricted Four Body Problem (CRFBP) is the problem of describing the dynamics of the motion of a "zero mass" body $P_S$ subject to the gravitational field generated by an assigned three body system ($P_1$, $P_2$ and $P_3$) on a two dimensional space. In this paper we analyze this problem with the additional assumption that the third

Primary $P_3$ has to be small enough such that it does not effect the motion of the other two massive bodies (and, for this reason, it will be identified hereafter with the generic name of "Asteroid").
The position of the Asteroid is set to correspond to one of the triangular Lagrangian points of the $P_1 - P_2 - Spacecraft$ Restricted Three Body System, which means that the Primaries form an equilateral triangle. It is well known, in fact, that these points are stable for values of the mass parameter $\mu$ smaller than Routh's critical mass $\frac{-9\pm\sqrt{69}}{18}$ in non-dimensional units [15].

Moreover the orbits of the three Primaries are taken to be circular, revolving around the barycenter of $P_1$ and $P_2$ with constant angular velocity $\omega$ such that, choosing a frame of reference $O_{x,y}$, centered in the center of rotation and revolving with the same angular velocity $\omega$ of the bodies, the three masses are fixed. The units of distance and mass are then scaled with the distance between $P_1$ and $P_2$ and the sum of their masses respectively, while the gravitational constant $\mathcal{G}$ and the rotational velocity $\omega$ are set to be one.
In this non dimensional units let $\mu$, $1-\mu$ and $\epsilon$ be the scaled mass of $P_2$, $P_1$ and $P_3$ respectively:

$$\begin{aligned}\mu &= \tfrac{m_2}{m_1+m_2}\\ 1-\mu &= \tfrac{m_1}{m_1+m_2}\\ \epsilon &= \tfrac{m_3}{m_1+m_2}\end{aligned}$$

As the planets are fixed and the origin of the system of reference is set in the barycenter of the major primaries, we can, without loss of generality, take the position of $P_1$ and $P_2$ to be $(-\mu, 0)$ and $(1-\mu, 0)$ respectively, which implies that the position of the Asteroid (see [16]) must be $(L_x, L_y) = (\frac{1}{2} - \mu, \frac{\sqrt{3}}{2})$ as in Fig.1.

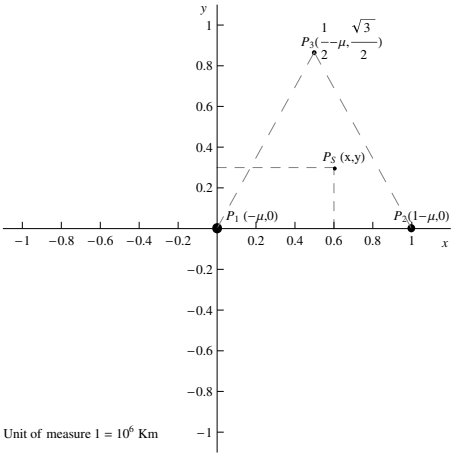


Figure 1: The Autonomous Coplanar CRFBP; in a rotating frame of reference, the planets are fixed and form an equilateral triangle.

The dynamics of the massless spacecraft (whose position is expressed in non-dimensional cartesian coordinates $x, y$) is described by the system:

$$\begin{cases} \ddot{x} = 2\dot{y} - \frac{\partial \Omega}{\partial x} \\ \ddot{y} = -2\dot{x} - \frac{\partial \Omega}{\partial y} \end{cases} \tag{1}$$

were the *augmented* or *effective* potential is:

$$\Omega = -\frac{x^2+y^2}{2} - \frac{(1-\mu)}{r_1} - \frac{\mu}{r_2} - \frac{\epsilon}{r_3}$$

the distance of the spacecraft from each of the three primaries is:

$$\begin{aligned} r_1 &= \sqrt{(x+\mu)^2 + y^2} \\ r_2 &= \sqrt{(x+\mu-1)^2 + y^2} \\ r_3 &= \sqrt{(x-L_x)^2 + (y-L_y)^2} \end{aligned}$$

$\frac{\partial \Omega}{\partial x}$ ($\frac{\partial \Omega}{\partial y}$), denotes the partial derivative of $\Omega$ with respect to $x$ ($y$), while the "dot" denotes the differentiation with respect to time.

In order to find the equilibrium points of the system, the velocities $\dot{x},\ \dot{y}$ and the accelerations $\ddot{x},\ \ddot{y}$ are set to be zero in (1) obtaining:

$$\begin{cases} \frac{\partial \Omega}{\partial x} = 0 \\ \frac{\partial \Omega}{\partial y} = 0 \end{cases} \tag{2}$$

Or equivalently

$$\begin{cases} x - \frac{(1-\mu)(x+\mu)}{\sqrt{(x+\mu)^2+y^2}^3} - \frac{\mu(x-(1-\mu))}{\sqrt{(x-(1-\mu))^2+y^2}^3} \\ \quad - \frac{\epsilon(x-L_x)}{\sqrt{(x-L_x)^2+(y-L_y)^2}^3} = 0 \\ y - \frac{(1-\mu)y}{\sqrt{(x+\mu)^2+y^2}^3} - \frac{\mu y}{\sqrt{(x-(1-\mu))^2+y^2}^3} \\ \quad - \frac{\epsilon(y-L_y)}{\sqrt{(x-L_x)^2+(y-L_y)^2}^3} = 0 \end{cases} \tag{3}$$

The green, continuous and the blue, dashed lines in Figure 2 represents the first and the second equation of system (3) respectively; the two lines intersect only six times forming the equilibrium points of the system as it would become clear zooming in as in Figure 3.

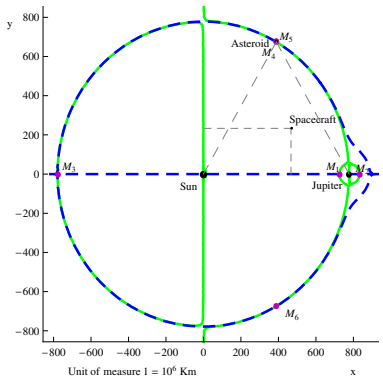


Figure 2: Equilibrium Points; the six intersections of the lines are the solutions of system (3): the equilibrium points of the system.

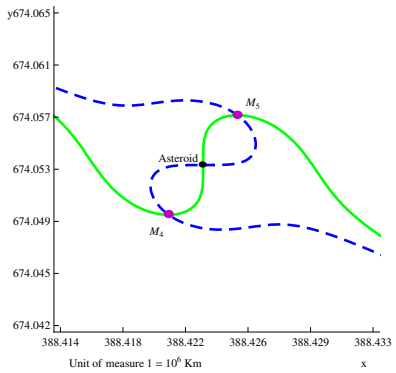


Figure 3: Equilibrium Points; zooming on the Asteroid and the two equilibrium points close to it.

The qualitative dynamics close to the asteroid do not change for different masses $\epsilon \in (0, \mu)$ of the Asteroid in that there are always two equilibrium points configured approximately at the same angle relative to the asteroid. However, quantitatively, as the mass increases the equilibrium points are displaced further from the asteroid, as shown in Figure 4. Thus, we would conclude that the only assumption on the mass of the Asteroid is that it has to be small enough such that it does not affect the motion of the other two Primaries.

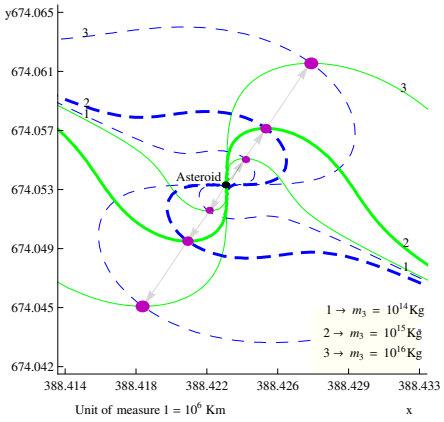


Figure 4: Equilibrium Points; $\forall \epsilon \in (0, \mu)$ the two lines intersects twice in the region close to the Asteroid.

Hereafter, for simplicity of notation, $(x_e, y_e)$ will indicate a generic equilibrium solution of system (3).

## III. STABILITY ANALYSIS

For the stability analysis a translation of the coordinates to the generic equilibrium point $(x_e, y_e)$ is performed.

$$\begin{cases} x' = x - x_e \\ y' = y - y_e \end{cases} \tag{4}$$

For simplicity of notation the indices above $x'$ and $y'$

are ignored.
The linearized motion close to the point $(x_e, y_e)$ is:

$$\begin{cases} \dot{x} = v_x \\ \dot{y} = v_y \\ \dot{v_x} = 2v_y + \alpha x + \chi y \\ \dot{v_y} = -2v_x + \chi x + \beta y \end{cases} \tag{5}$$

with

$$\alpha = 1 + \frac{(1-\mu)\left[2(x_e+\mu)^2 - {y_e}^2\right]}{\sqrt{(x_e+\mu)^2+y_e^2}^5} + \frac{\mu\left[2(x_e+\mu-1)^2 - {y_e}^2\right]}{\sqrt{(x_e+\mu-1)^2+y_e^2}^5} + \frac{\epsilon\left[2(x_e-L_x)^2 - (y_e-L_y)^2\right]}{\sqrt{(x_e-L_x)^2+(y_e-L_y)^2}^5}$$

$$\beta = 1 + \frac{(1-\mu)\left[-(x_e+\mu)^2 + 2{y_e}^2\right]}{\sqrt{(x_e+\mu)^2+y_e^2}^5} + \frac{\mu\left[-(x_e+\mu-1)^2 + 2{y_e}^2\right]}{\sqrt{(x_e+\mu-1)^2+y_e^2}^5} + \frac{\epsilon\left[-(x_e-L_x)^2 + 2(y_e-L_y)^2\right]}{\sqrt{(x_e-L_x)^2+(y_e-L_y)^2}^5}$$

$$\chi = 3\left\{ \frac{(1-\mu)[(x_e+\mu)y_e]}{\sqrt{(x_e+\mu)^2+y_e^2}^5} + \frac{\mu[(x_e+\mu-1)y_e]}{\sqrt{(x_e+\mu-1)^2+y_e+^2}^5} + \frac{\epsilon\left[(x_e-L_x)(y_e-L_y)\right]}{\sqrt{(x_e-L_x)^2+(y_e-L_y)^2}^5} \right\}$$

Therefore the four eigenvalues of the system are:

$$\begin{aligned} \Psi_{1,2} &= \pm\sqrt{\frac{-(4-\alpha-\beta)+\sqrt{(4-\alpha-\beta)^2-4\alpha\beta+4\chi^2}}{2}} \\ \Psi_{3,4} &= \pm\sqrt{\frac{-(4-\alpha-\beta)-\sqrt{(4-\alpha-\beta)^2-4\alpha\beta+4\chi^2}}{2}} \end{aligned} \tag{6}$$

It can be shown that, fixing a specific mass $\epsilon \in (0, \mu)$ for the Asteroid, and evaluating the eigenvalues corresponding to both the equilibrium points, only one of them will have positive Real part, which implies that the natural equilibrium points are both $saddle \times center$ points, i.e. linearly unstable, and therefore nonlinearly unstable.

Evaluating the eigenvalues for the Sun-Jupiter-Trojan Asteroid-Spacecraft system, where the mass of the Asteroid is set to be $10^{15}Kg$ (reasonable, since the total mass of all the Trojan Asteroids is equal to $0.0001$ times the mass of the Earth $\sim 5.9736\times10^{20}Kg$). Then, as expected, both the equilibrium points $M_4$ and $M_5$ are unstable.
In particular, in non dimensional units, evaluating them in $M_4 = (M_{4_x}, M_{4_y}) = (0.499044; 0.866021)$ yields:

$$\begin{aligned} \Psi_{1,2} &= \pm 2.07049 \\ \Psi_{3,4} &= \pm 2.50695i \end{aligned}$$

While for $M_5 = (M_{5_x}, M_{5_y}) = (0.499049; 0.86603)$ we find:

$$\begin{aligned} \Psi_{1,2} &= \pm 2.07047 \\ \Psi_{3,4} &= \pm 2.50693i \end{aligned}$$

## IV. THE LOW-THRUST AUTONOMOUS COPLANAR CRFBP

The idea of this paper is to investigate the dynamics of a low-thrust spacecraft in the Autonomous Coplanar CRFBP. Using the thrust propulsion our spacecraft can create artificial equilibrium points suitable for Asteroid observation missions. In addition a subset of these novel equilibrium points are proved to be stable such that the motion will remain bounded in a small region about them, with relatively low fuel requirements and without the need for a state feedback control.

Given a maximum thrusting capability $\mathcal{F}$ expressed in $mN$, which can be developed by the spacecraft, and an approximate weight for the spacecraft $W_s$, evaluated in Tons, the maximal acceleration in the non-dimensional units is given by:

$$\begin{aligned} a_{_{nondim}} &= \frac{\mathcal{F}}{W_s}\frac{mN}{T} = \frac{\mathcal{F}\times10^{-6}}{W_s}\cdot\frac{m}{s^2} \\ &= \frac{\mathcal{F}\times10^{-6}}{W_s}\cdot\frac{Kg}{m^2}\frac{m^3}{Kg\cdot s^2} \\ &= \frac{\mathcal{F}\times10^{-6}}{W_s}\frac{d^2_{P_1/P_2}}{(m_1+m_2)}\frac{1}{\mathcal{G}} \end{aligned} \tag{7}$$

where $d_{P_1/P_2}$ means the distance in meters between the two major Primaries.
Indicating the acceleration with $a\hat{\mathbf{n}} = a_x\bar{\mathbf{x}} + a_y\bar{\mathbf{y}}$ where $a = \sqrt{a_x^2 + a_y^2}$ is the magnitude and $\hat{\mathbf{n}}$ is the direction of the acceleration itself, $a$ will therefore be contained in $(0; a_{_{nondim}})$.

As mentioned in previous sections, an optimistic but realistic, "near term", reachable maximal thrusting power $\mathcal{F}$ is taken to be $300mN$.
In order to estimate the range of possible acceleration on the spacecraft we fix it's mass to be $1T$.
For the Sun-Jupiter-Trojan Asteroid-Spacecraft system the non-dimensional value of the maximum acceleration $a_{nondim}$ will therefore be $1.36765$.

Moreover the acceleration has to be constant in the direction of the perturbation, namely

$$\frac{\partial}{\partial x}(a\hat{\mathbf{n}}) = \frac{\partial}{\partial y}(a\hat{\mathbf{n}}) = 0 \tag{8}$$

Adding low-thrust to system (1) it becomes:

$$\begin{cases} \ddot{x} = 2\dot{y} - \frac{\partial\Omega}{\partial x} + a_x \\ \ddot{y} = -2\dot{x} - \frac{\partial\Omega}{\partial y} + a_y \end{cases} \tag{9}$$

with

$$\Omega = -\frac{x^2+y^2}{2} - \frac{(1-\mu)}{r_1} - \frac{\mu}{r_2} - \frac{\epsilon}{r_3}$$

$$a = \sqrt{a_x^2 + a_y^2} \leq a_{_{nondim}}$$

$$\begin{aligned} r_1 &= \sqrt{(x+\mu)^2+y^2} \\ r_2 &= \sqrt{(x+\mu-1)^2+y^2} \\ r_3 &= \sqrt{(x-L_x)^2+(y-L_y)^2} \end{aligned}$$

Again, to find the equilibrium points, the velocities $\dot{x}, \dot{y}$ and the accelerations $\ddot{x}, \ddot{y}$ are set to be zero in (9), obtaining:

$$\begin{cases} a_x = \frac{\partial \Omega}{\partial x} \\ a_y = \frac{\partial \Omega}{\partial y} \end{cases} \tag{10}$$

That can also be seen as:

$$\begin{cases} a = |\nabla \Omega| \\ \hat{\mathbf{n}} = -\frac{\nabla \Omega}{|\nabla \Omega|} \end{cases} \tag{11}$$

System (11) states that, in order to get a new equilibrium point, the acceleration on the spacecraft due to the thrusters has to be equal in magnitude (first equation) but opposite in direction (second equation) to the acceleration on the spacecraft due to the gravitational field at that point.

## V. STABILITY ANALYSIS OF THE LINEARIZED SYSTEM

Notice that, with a constant thrust, system (9), once linearized, is equal to the linear system in (5) and therefore the linear stability of the equilibrium points resulting from system (11) will be given by the analysis of the eigenvalues in (6).

By the Lyapunov Stability theorem (see for example [17]), in order to obtain a linearly bounded motion, the eigenvalues must have Real part less than or equal to zero. In our case, recall (6), we cannot have a non zero Real part, as it would imply that $Re(\Psi_1) > 0$ or $Re(\Psi_2) = Re(-\Psi_1) = -Re(\Psi_1) > 0$ and/or the same for $\Psi_3, \Psi_4$, thus leading to a $saddle \times saddle$ or a $saddle \times center$ unstable equilibrium point respectively.
Therefore, in this case, it is only possible to have linearly bounded motion where $Re(\Psi_k) = 0$, $k = 1, 2, 3, 4$

Thus, recalling (6), the conditions for the four eigenvalues to be purely Imaginary are:

$$\begin{cases} (4-\alpha-\beta)^2 - 4\alpha\beta + 4\chi^2 \geq 0 \\ -(4-\alpha-\beta) + \sqrt{(4-\alpha-\beta)^2 - 4\alpha\beta + 4\chi^2} \leq 0 \end{cases} \tag{12}$$

System (12) is satisfied by the "stable zone" of Figure 5.
In particular the first inequality of the system is verified by the points outside the dark-green, dashed line, while the second by those outside the green, continuous line. The intersection of these two zones, namely the external part of the "four leaf clover" zone, is then the area in which the linearized motion is stable. Notice that, as shown before, the equilibrium points $M_4$ and $M_5$ are linearly unstable.

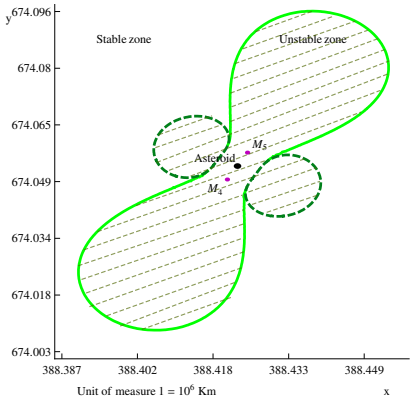


Figure 5: Linearly stable-unstable zones; system (12) is satisfied by the points outside the "four leaf clover", the linearly stable zone.

Of course there exist an external limit of the linearly stable zone as represented in Figure 6. In particular the first inequality of the system is verified by the points between the dark-green, dashed lines, while the second by those between the green, continuous lines. The intersection of these two zones is then the actual area in which the linearized motion is stable.

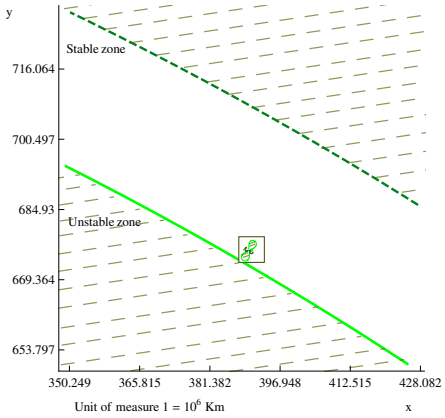


Figure 6: The external stability boundary of the linearly stable zone;(for displaying purpose the zone inside the square is magnified by $\sim 50$ times).

In the Sun-Jupiter-Trojan Asteroid-Spacecraft system, the maximal possible thrust to remain within the stability boundary will approximately be of magnitude $0.4826mN$.
Anyway, in this paper, the actual thrust used is lower than $10\mu N$, that will enable to create artificial equilibrium points in the area between the two dark, purple lines in Figure 7.

Four artificial equilibrium points $A$, $B$, $C$, $D$ are chosen in the linearly stable zone, at a distance from the

unstable zone equal or higher than $2000km$ (see Figure 7), since we want to remain as close as possible to the Asteroid but far enough from the unstable zone, such that even with injection errors the spacecraft will remain in the stable zone (see Fig 7).

For the Sun-Jupiter-Trojan Asteroid-Spacecraft system the four points are at a distance of approximately $15000km$ from the Asteroid.

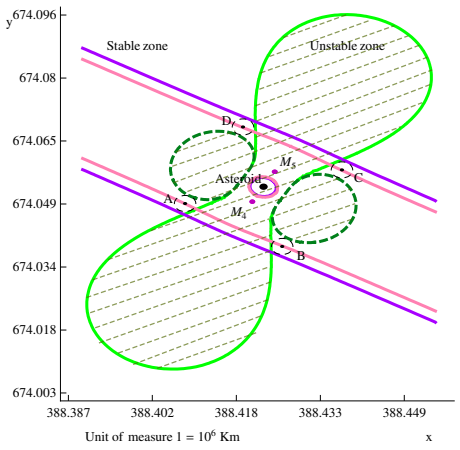


Figure 7: Adding the low-thrust; using a thrust lower than $10\mu N$, four equilibria $A$, $B$, $C$, $D$ are created in the stable zone, reachable with a thrust $\sim 0.0089mN$.

To evaluate the thrust required to create an artificial equilibrium point, for example in $A = (A_x; A_y)$, the computation of the gravitational field in this point is needed.
In the Sun-Jupiter-Trojan Asteroid-Spacecraft system, in non-dimensional units, it is:

$$\begin{aligned} a_x &= -A_x + \frac{(1-\mu)(A_x+\mu)}{\sqrt{(A_x+\mu)^2+A_y^2}^3} + \frac{\mu(A_x+\mu-1)}{\sqrt{(A_x+\mu-1)^2+A_y^2}^3} \\ &\quad + \frac{\epsilon(A_x-L_x)}{\sqrt{(A_x-L_x)^2+(A_y-L_y)^2}^3} \\ &= -0.0000195028 \end{aligned}$$

$$\begin{aligned} a_y &= -A_y + \frac{(1-\mu)A_y}{\sqrt{(A_x+\mu)^2+A_y^2}^3} + \frac{\mu A_y}{\sqrt{(A_x+\mu-1)^2+A_y^2}^3} \\ &\quad + \frac{\epsilon(A_y-L_y)}{\sqrt{(A_x-L_x)^2+(A_y-L_y)^2}^3} \\ &= -0.000035642 \end{aligned} \tag{13}$$

Such that the magnitude of required thrust is:

$$a = \sqrt{a_x^2 + a_y^2} = 0.0000406289 (\sim 0.0089mN) \tag{14}$$

This thrust is represented by the pink line in Figure 7 and, as we can clearly see, it is approximately the same thrust required to create the other three equilibrium points $B$, $C$ and $D$.
We will analyze in detail the motion for $A$, since all the four points have similar behaviors as we will show graphically later on.

## VI. INTEGRATING THE LINEARIZED MOTION

Calling $\mathcal{A}$ the Jacobian matrix corresponding to system (5), namely:

$$\mathcal{A} = \begin{pmatrix} 0 & 0 & 1 & 0 \\ 0 & 0 & 0 & 1 \\ \alpha & \chi & 0 & 2 \\ \chi & \beta & -2 & 0 \end{pmatrix} \tag{15}$$

The eigenvectors of the system are four vectors $\mathbf{f_j} \in \mathbb{C}^4$, $j = 1, ..., 4$ such that

$$\mathcal{A}\mathbf{f_j} = \Psi_j \mathbf{f_j}, \quad j = 1, ..., 6 \tag{16}$$

Recalling that linearizing the system (9) yields the linear system (5), whose eigenvalues are those in (6), we take an equilibrium point within the linearly stable zone (i.e. with purely imaginary eigenvalues), and thus rearrange the eigenvalues in the form:

$$\begin{aligned} \Psi_1 &= \lambda i \\ \Psi_2 &= -\lambda i \\ \Psi_3 &= \nu i \\ \Psi_4 &= -\nu i \end{aligned} \tag{17}$$

where

$$\begin{aligned} \lambda &= \sqrt{\frac{(4-\alpha-\beta)-\sqrt{(4-\alpha-\beta)^2-4\alpha\beta+4\chi^2}}{2}} \\ \nu &= \sqrt{\frac{(4-\alpha-\beta)+\sqrt{(4-\alpha-\beta)^2-4\alpha\beta+4\chi^2}}{2}} \end{aligned} \tag{18}$$

$\lambda, \mu \in \mathbb{R}$.

Being the eigenvalues two couples of complex conjugated values, the eigenvectors must be conjugated too, namely $\mathbf{f_2} = \mathbf{f_1}^*$ and $\mathbf{f_4} = \mathbf{f_3}^*$, and therefore we need just to find $\mathbf{f_1}$ and $\mathbf{f_3}$.

With a few algebraic manipulations it is possible to calculate their explicit expressions:

$$\begin{aligned} \mathbf{f_1} &= [1, -\tfrac{\chi}{\beta+\lambda^2}, 0, -\tfrac{2\lambda^2}{\beta+\lambda^2}]^T \\ &\quad + i[0, \tfrac{2\lambda}{\beta+\lambda^2}, \lambda, -\tfrac{\chi\lambda}{\beta+\lambda^2}]^T \\ \mathbf{f_3} &= [1, -\tfrac{\chi(\alpha+\nu^2)}{\chi^2+4\nu^2}, 0, -\tfrac{2\nu^2(\alpha+\nu^2)}{\chi^2+4\nu^2}]^T \\ &\quad + i[0, \tfrac{2\nu(\alpha+\nu^2)}{\chi^2+4\nu^2}, \nu, -\tfrac{\chi\nu(\alpha+\nu^2)}{\chi^2+4\nu^2}]^T \end{aligned} \tag{19}$$

The matrix $\mathcal{M}$ of the change of coordinates which diagonalize $\mathcal{A}$ will therefore be:

$$\mathcal{M} = \begin{pmatrix} 1 & 0 & 1 & 0 \\ -\frac{\chi}{\beta+\lambda^2} & \frac{2\lambda}{\beta+\lambda^2} & -\frac{\chi(\alpha+\nu^2)}{\chi^2+4\nu^2} & \frac{2\nu(\alpha+\nu^2)}{\chi^2+4\nu^2} \\ 0 & \lambda & 0 & \nu \\ -\frac{2\lambda^2}{\beta+\lambda^2} & -\frac{\chi\lambda}{\beta+\lambda^2} & -\frac{2\nu^2(\alpha+\nu^2)}{\chi^2+4\nu^2} & -\frac{\chi\nu(\alpha+\nu^2)}{\chi^2+4\nu^2}) \end{pmatrix} \tag{20}$$

Applying the transformation of coordinates $\mathcal{M}^{-1}$ on $\mathrm{x} = [x, y, v_x, v_y]^T$, yields the new coordinates $\mathfrak{J} = [\xi_1, \xi_2, \psi_1, \psi_2]^T$, namely:

$$\mathfrak{J} = \mathcal{M}^{-1}\mathrm{x} \tag{21}$$

The transformation $\mathcal{M}$ is performed on the system (5) to find it's expression in the new coordinates:

$$\dot{\mathfrak{J}} = \mathcal{M}^{-1}\dot{\mathrm{x}} = \mathcal{M}^{-1}\mathcal{A}\,\mathrm{x} = \mathcal{M}^{-1}\mathcal{A}\,\mathcal{M}\,\mathfrak{J} \tag{22}$$

that can be rewritten as:

$$\dot{\mathfrak{J}} = \mathcal{A}'\,\mathfrak{J} \;\; with \;\; \mathcal{A}' = \mathcal{M}^{-1}\mathcal{A}\,\mathcal{M} \tag{23}$$

Where $\mathcal{A}'$ is:

$$\mathcal{A}' = \begin{pmatrix} 0 & \lambda & 0 & 0 \\ -\lambda & 0 & 0 & 0 \\ 0 & 0 & 0 & \nu \\ 0 & 0 & -\nu & 0 \end{pmatrix} \tag{24}$$

Calling $\mathfrak{J}_0 = [\xi_1^0, \xi_2^0, \psi_1^0, \psi_2^0]^T$ the array of the initial conditions of system (23), its solutions will be:

$$\mathfrak{J}(t) = \mathfrak{J}_0 e^{\mathcal{A}'t} \tag{25}$$

For the well known properties of the exponential of a matrix, system (25) can be rewritten in a coordinate form as:

$$\begin{cases} \xi_1(t) = \cos(\lambda t)\xi_1^0 + \sin(\lambda t)\xi_2^0 \\ \xi_2(t) = \cos(\lambda t)\xi_2^0 - \sin(\lambda t)\xi_1^0 \\ \psi_1(t) = \cos(\nu t)\psi_1^0 + \sin(\nu t)\psi_2^0 \\ \psi_2(t) = \cos(\nu t)\psi_2^0 - \sin(\nu t)\psi_1^0 \end{cases} \tag{26}$$

Therefore the solution of system (9), given by $\mathrm{x}(t) = \mathcal{M}\mathfrak{J}(t)$, are:

$$\begin{cases} x(t) = \xi_1^0\cos(\lambda t) + \xi_2^0\sin(\lambda t) + \psi_1^0\cos(\nu t) \\ \qquad +\psi_2^0\sin(\nu t) \\ y(t) = -\frac{c}{\lambda^2+b}(\xi_1^0\cos(\lambda t) + \xi_2^0\sin(\lambda t)) \\ \qquad +\frac{2\lambda}{\lambda^2+b}(\xi_2^0\cos(\lambda t) - \xi_1^0\sin(\lambda t)) \\ \qquad -\frac{c(\nu^2+a)}{c^2+4\nu^2}(\psi_1^0\cos(\nu t) + \psi_2^0\sin(\nu t)) \\ \qquad +\frac{2\nu(\nu^2+a)}{c^2+4\nu^2}(\psi_2^0\cos(\nu t) - \psi_1^0\sin(\nu t)) \end{cases} \tag{27}$$

Notice that, evaluating $x(0)$, $y(0)$, $v_x(0) = \dot{x}(0)$ and $v_y(0) = \dot{y}(0)$, as expected, yields:

$$\begin{pmatrix} x(0) \\ y(0) \\ v_x(0) \\ v_y(0) \end{pmatrix} = \mathcal{M}\begin{pmatrix} \xi_1^0 \\ \xi_2^0 \\ \psi_1^0 \\ \psi_2^0 \end{pmatrix} \tag{28}$$

which is equal to (21) evaluated at $t = 0$.

These resulting orbits, solution of the linearized system, are expressed in the system of reference translated to the artificial equilibrium point $x_e$, $y_e$ (recall (4)) such that they must be translated back to the barycenter of $P_1$ and $P_2$.

a) after 1 Jovian year ($\sim$ 12 Terrestrial years)

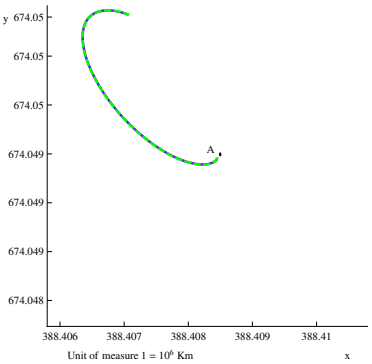


b) after 2 Jovian years ($\sim$ 24 Terrestrial years)

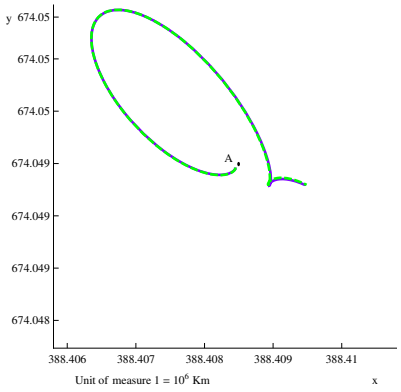


c) after 12 Jovian year ($\sim$ 150 Terrestrial years)

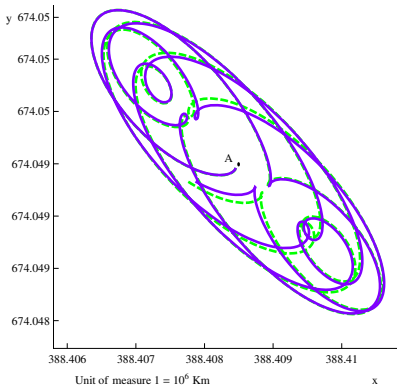


Figure 8: The solution of the linearized system; the purple, continuous line is the analytic solution of the linearized system while the green, dashed line is the numerical integration of the linearized system.

The behavior of the analytic solution of the linearized system, as shown by the purple, continuous line in Figure 8 a), b), c), starting sufficiently close to the point A, remains, as expected, bounded close to the initial point for a long period of time.
Just as a check, in the same graph the numerical integration is also performed represented by the green, dashed line. As expected the numerical error (i.e. the distance between the two solutions), although small, increases with time confirming the analytical solution and underlining the limits of the numerical method.

## VII. INTEGRATING THE FULL NONLINEAR SYSTEM

The next, final step is to investigate the full nonlinear system in (9) and perform a numerical integration with Mathematica using a Runge Kutta method, starting sufficiently close to our point A. The result of the integration, when starting with a null initial velocity, is shown by the blue line in Figure 9.
The light purple, dashed line in the graph is, once more, the analytic solution of the linearized system. The comparison of the two solutions underlines that, although quantitatively different, the qualitative dynamics behave in a similar, bounded way. As a result

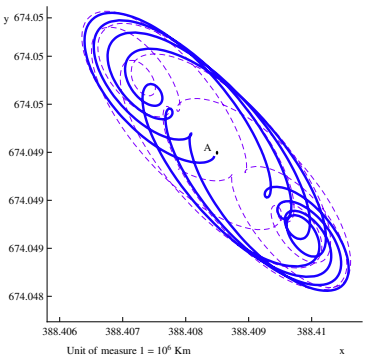


Figure 9: The bounded orbit around A; the blue, continuous line is the numerical integration of the nonlinear system, the purple, dashed line is the analytic solution of the linearized system.

of the application of the same method to the points $B$, $C$ and $D$, the other three orbits are determined that, starting sufficiently close to each point, remain bounded around it.
In particular, for each of the four points, the motion remains within the $2000km$ circular domain outside the unstable zone as in Figures 10 and 11.

At last notice that, considering the couples A-C and B-D, the behavior of the orbits in each couple is very similar and furthermore the motion of the second couple is bounded in an area smaller than the $2000km$.

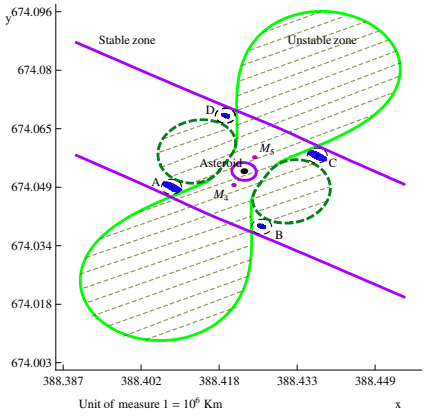


Figure 10: The resulting orbits; thrusting $\sim 0.009mN$, each orbit remains in the $2000km$ domain.

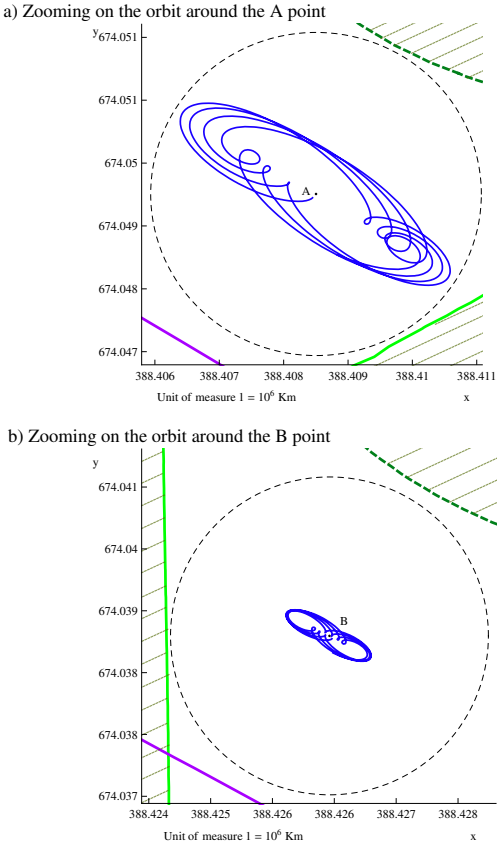

c) Zooming on the orbit around the C point

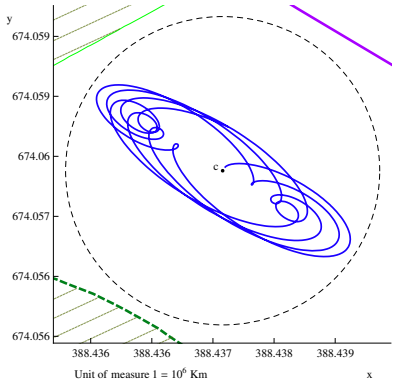


d) Zooming on the orbit around the D point

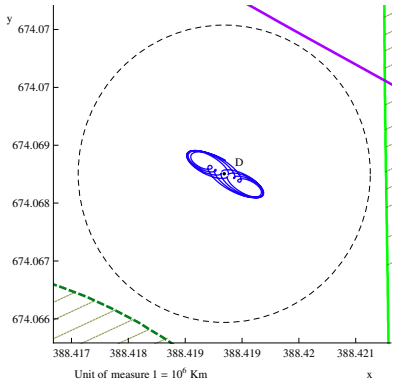


Figure 11: The four resulting bounded orbits; starting close to each point we will remain within the $2000km$ circular domain outside the unstable zone.

## VIII. SUMMARY

An Autonomous Coplanar CRFBP has been formulated for both the purpose of mathematical interest as well as to investigate potential applications in the Sun-Jupiter-Trojan Asteroid-Spacecraft system.

A stability analysis of the linearized motion reveals that the natural equilibrium points of the system are unstable. A constant low-thrust is added to the spacecraft, which can generate a thrust up to $300mN$. It is then shown that a region of stable artificial equilibrium points close to the Asteroid can be created using this low-thrust propulsion.

As a result completely novel, bounded orbits are proved to exist, that in the Sun-Jupiter-Trojan Asteroid-Spacecraft system can be maintained with a constant thrust lower than $10\mu N$ oriented in a fixed direction. Furthermore these orbits remain within a $2000km$ circular domain inside the linearly stable zone and approximately $15000km$ from the Asteroid.

In summary the possibility to maintain, with limited fuel requirements, strategic, observational positions close to an Asteroid is illustrated. This requirement is of huge importance for any discovery mission either for observational, scientific or commercial fields.

# References


[1] Scheeres, D. J. 'The Restricted Hill Four-Body Problem with Applications to the Earth Moon Sun System'. *Celestial Mechanics and Dynamical Astronomy*, Vol. 70, No. 2 :pp. 75–98, 1998.

[2] Cronin, J., Richards, P. B., Russell, L. H. 'Some periodic solutions of a four-body problem'. *Icarus*, Vol.3:pp. 423, 1964.

[3] Michalodimitrakis, M. 'The circular restricted four body problem'. *Astrophysics and Space Science*, Vol. 75, No.2 :pp. 289–305, 1981.

[4] Papadakis, K. E. 'Asymptotic orbits in the restricted four body problem'. *Planetary and Space Science*, Vol. 55, No. 10 :pp. 1368–1379, 2007.

[5] Morimoto, K., Yamakawa, M. Y., Uesugi, H. 'Artificial Equilibrium Points in the Low-Thrust Restricted Three-Body Problem'. *Journal of Guidance, Control, and Dynamics*, Vol. 30, No. 5 :pp. 1563–1568, 2007.

[6] McInnes, C. R., McDonald, A. J., John, F. L., MacDonald, E. W. ' Solar sail parking in restricted three-body systems'. *Journal of Guidance, Control, and Dynamics*, Vol. 17, No. 2 :pp. 399–406, 1994.

[7] Baig, S., McInnes, C. R. 'Artificial Three Body Equilibria for Hybrid Low-Thrust Propulsion'. *Journal of Guidance, Control, and Dynamics*, Vol. 31, No. 6 :pp. 1644–1655, 2008.

[8] Morimoto, K., Yamakawa, M. Y., Uesugi, H. 'Periodic Orbits with Low-Thrust Propulsion in the Restricted Three-Body Problem '. *Journal of Guidance, Control, and Dynamics*, Vol. 29, No. 5 :pp. 1131–1139, 2006.

[9] Waters, T., McInnes, C. R. 'Periodic orbits above the ecliptic plane in the solar sail restricted 3-body problem'. *Journal of Guidance, Control, and Dynamics*, Vol. 30, No. 3 :pp. 687–693, 2007.

[10] Baig, S., McInnes, C. R. 'Artificial halo orbits for low-thrust propulsion spacecraft'. *Celestial Mechanics and Dynamical Astronomy*, Vol. 104, No. 4 :pp. 321–335, 2009.

[11] McKay, R., Macdonald, M., Bosquillon de Frescheville, F., Vasile, M., McInnes, C.R., Biggs, J. ' Non-Keplerian Orbits Using Low Thrust, High ISP Propulsion Systems'. In *60th International Astronautical Congress*, 2009.

[12] Wallace, N. C. 'Testing of the QinetiQ T6 thruster in support of the ESA Bepicolombo Mercury mission'. In *Proceedings of the 4th International Spacecraft Propulsion Conference (ESA SP-555)*, 2004.

[13] Shoemaker, E. M., Shoemaker, C. S., Wolfe, R. F. 'Trojan asteroids: populations, dynamical structure and origin of the L4 and L5 swarms'. In *Asteroids II, Proceedings of the Conference, Tucson, AZ*, 1988.

[14] Rivkin, A. S., Emery, J., Barucci, A., Bell, J. F., Bottke, W. F., Dotto, E., Gold, R., Lisse, C., Licandro, J., Prockter, L., Hibbits, C., Paul, M., Springmann, A., Yang, B. 'The Trojan Asteroids: Keys to Many Locks'. *SBAG Community White Papers*, 2009.

[15] Deprit, A., Deprit-Bartholome, A. 'Stability of the triangular Lagrangian points'. *Astronomical Journal*, Vol.72:pp. 173, 1967.

[16] Ambrosetti, A., Prodi, G. *'A Primer of Nonlinear Analysis '*. Cambridge University Press, 1993.

[17] Arnold, V. A., Kozolov, V. V, Neishtadt, A. I. *'Mathematical aspects of classical and celestial mechanics. (Dynamical systems. III)'*. Springer-Verlag, 2006.

[18] Conley, C. C. 'Low Energy Transit Orbits in the Restricted Three Body Problem'. *SIAM Journal on Applied Mathematics*, Vol. 16, No. 4 :pp. 732–746, 1968.

[19] Koon, W. S., Lo, M., Marsden, J. E., Ross. S. *'Dynamical Systems, the Three-Body Problem and Space Mission Design'*. Marsden Books, 2008.

[20] Szebehely,V. *'Theroy of Orbits'*. Academic Press, 1697.